22nd International Conference on Sustainable Energy Technologies
Kuala Lumpur, Malaysia, 13 to 15 August 2026 · ISBN 978-1-995850-00-9 · ISSN 2978-4387

CONFERENCE PAPER · ENERGY STORAGE & CONVERSION

Experimental Investigation of the Effects of MXene Concentration and Optical Filter Layer Thickness on PV/T System Performance

Ziyan Sun[1*], Xianlong Shi[1], Yuanlong Cui[1]

[1] Shandong Jianzhu University, 1000 Fengming Road, Jinan, 250101, China

RECEIVED 15 April 2026 · REVISED 20 May 2026 · ACCEPTED 1 June 2026
PRESENTED 13 to 15 August 2026 · PUBLISHED 23 November 2026

ABSTRACT

Spectral filtering technology provides an effective approach for improving the thermal management capability and solar spectrum utilization of photovoltaic/thermal (PVT) systems by selectively regulating the distribution of solar radiation. However, excessive spectral absorption may reduce photovoltaic conversion performance, and the optimal balance between thermal recovery and electrical output remains unclear. In this study, a MXene-based spectral filtering PVT system was experimentally investigated by employing MXene nanofluids with different concentrations (0.0005 wt% and 0.001 wt%) and optical filter layer thicknesses (1, 3, and 5 cm). The effects of MXene concentration and optical thickness on photovoltaic performance, thermal energy recovery, and overall energy conversion efficiency were systematically evaluated. The results demonstrate that increasing optical filter thickness enhances solar spectral attenuation but reduces the effective solar radiation reaching the PV module, resulting in decreased electrical output. Similarly, increasing MXene concentration strengthens broadband solar absorption, but excessive nanoparticle loading causes stronger spectral blockage, which negatively affects photovoltaic performance. Among all tested configurations, the 1 cm thick 0.0005 wt% MXene filtering layer achieved the best balance between thermal and electrical performance, providing the highest overall efficiency of 41.37%, exceeding those of the water-based filter (39.35%) and the 0.001 wt% MXene filter (37.30%). The results indicate that the performance enhancement of MXene-based spectral filtering PVT systems is governed by the trade-off between spectral regulation and photovoltaic preservation. Appropriate optimization of MXene concentration and optical filter thickness is essential for maximizing solar energy utilization, improving thermal management, and achieving higher comprehensive energy conversion efficiency in next-generation PVT applications.

KEYWORDS Solar PV/T system, Optical filtration layer, Nanofluids, Thermal and electrical energy efficiency, Photovoltaic cell

1. Introduction

Solar energy is an abundant renewable resource with considerable potential to meet electricity and heating demands. Photovoltaic/thermal (PV/T) systems recover heat from PV cells while generating electricity, thereby improving the utilization of incident solar energy (Herrando *et al.* 2023). Their performance depends on both the solar spectrum reaching the cells and heat removal from the absorber. Optical filtration offers an additional means of controlling this energy distribution. A liquid filter can absorb part of the incident radiation before it reaches the PV surface, but attenuation within the useful PV response band can also reduce electrical generation (Cui *et al.* 2026; Jiao *et al.* 2024).

Liquid filters have been investigated using emulsions (Lee *et al.* 2023), water (Yadav *et al.* 2024), silver nanofluids (Wang *et al.* 2025), CNT/Ag mixtures (Xia *et al.* 2023), and magnetic nanofluids (Xing

* Corresponding author. Email address: 2024050206@stu.sdjzu.edu.cn (Ziyan Sun)

© 2026 The Author(s).
Published by Caravel Press.

doi.org/10.65582/set.2026.007

et al. 2024). MXene has attracted interest because of its optical absorption characteristics and light-to-heat conversion capability (Zeng *et al.* 2024). Recent research has also demonstrated the potential of MXene-based nanofluids to balance optical absorption, dispersion stability, and photothermal performance (Anwer *et al.* 2025). Studies using oil-based MXene nanofluids (Rubbi *et al.* 2020), MXene/water nanofluids (Wang *et al.* 2021), and MXene/methanol nanofluids (Dashtbozorg *et al.* 2025) provide evidence for their application in solar thermal conversion and PV/T thermal management. More directly, Cui *et al.* (2025) experimentally compared liquid optical filtration PV/T modules using different working fluids, in a subsequent study (Cui *et al.* 2026), they employed both numerical simulations and experimental validation to investigate the effects of the filtering layer thickness, MXene concentration, and operating conditions (Cui *et al.* 2026).

Despite the promising optical and thermal properties of MXene-based nanofluids, their application as spectral filtering media in PV/T systems remains insufficiently investigated. In particular, the relationship between the optical losses introduced by spectral regulation and the thermal benefits obtained from nanofluid cooling has not been fully clarified. Therefore, the authors developed a hybrid PV/T system incorporating MXene/water nanofluids as both optical filter layers (OFLs) and heat transfer fluids (HTFs). Uncovered monocrystalline silicon PV cells were employed to eliminate the influence of the conventional glass cover and accurately evaluate the intrinsic effects of the optical filter layers. The authors experimentally investigated the effects of MXene concentration (0.0005 wt% and 0.001 wt%) and optical filter layer thickness (1, 3, and 5 cm) on the electrical and thermal performance of the PV/T system under indoor conditions.

2. Materials and methods

2.1. Physical model of PV/T system

Figure 1 presents the structure of the PV/T module with OFL. The module consists of a liquid-based OFL fabricated from quartz glass, which exhibits a broadband transmittance of approximately 92% over the wavelength range of 350-2500 nm (Cai *et al.* 2025), a monocrystalline silicon PV cell, a serpentine copper tube bonded to the rear of the absorber and a layer of insulation at the bottom.

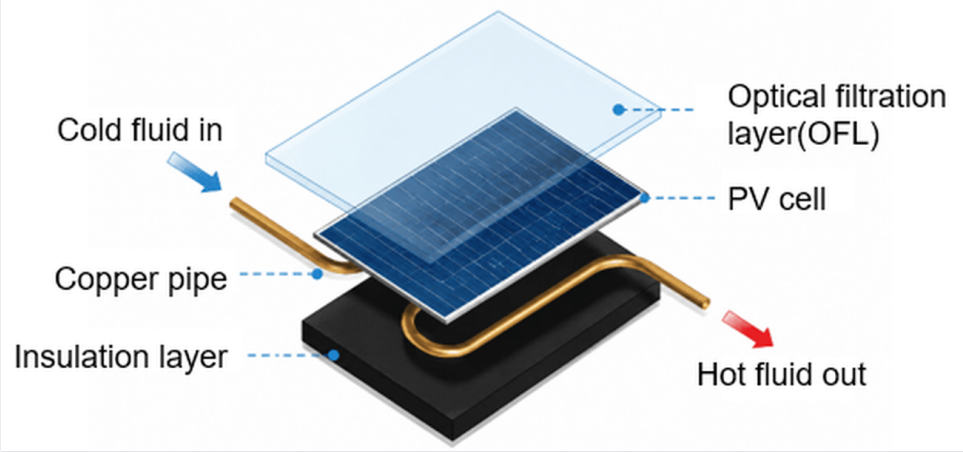

Figure 1. Schematic diagram of PV/T with OFL module.

The surface temperature of the module is influenced by direct solar radiation and heat exchange with the atmospheric environment. When solar radiation reaches the OFL surface, a portion of the ultraviolet portion is absorbed, and some radiation is absorbed or scattered within the OFL, while the remaining radiation passes through the OFL and reaches the PV surface. The nanofluids within the OFL exhibit unique optical properties as spectral filtering fluids, which depend on the optical characteristics of both the base fluid and the nanoparticles. The PV cell generates electricity under solar irradiation while its temperature rises. Heat is removed from the cell by the heat transfer fluid

circulating through the copper tube, while the bottom insulation layer reduces heat loss to the surroundings.

2.2. MXene nanofluid preparation and physical properties

Based on existing research, a two-step method is used to prepare the stable MXene nanofluids (Sanjeevi and Loganathan 2020). Figure 2 illustrates the preparation process of MXene/water nanofluid: (i) MXene powder and trisodium citrate dihydrate (TCD) surfactant as 1:3 ratio is added to de-ionized water (DI-water); (ii) the mixture is stirred on a magnetic stirrer at 600 rpm for 30 minutes to obtain a uniform liquid; (iii) the mixture liquid is placed under an ultrasonic probe (FS-1200N) with 4/6 s on/off pulsing for 2 hours to obtain the MXene/water solution.

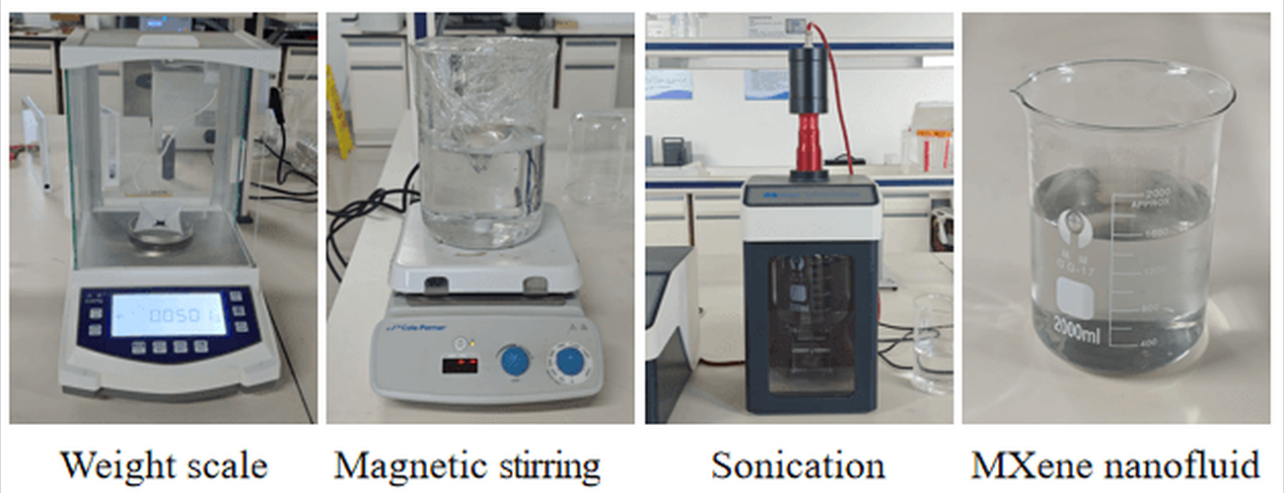

Figure 2. Two-step method MXene nanofluid preparation actual pictures.

SEM and EDS were used to examine the morphology and elemental distribution of samples from the same batch. SEM imaging was performed at 5 kV and 25 ± 2 °C. The SEM result reveals a typical accordion-like layered structure of MXene nanosheets, confirming the successful exfoliation of the MAX precursor into two-dimensional layers. EDS confirms the presence of Ti, C and Cl elements, verifying the Ti-C framework of $Ti_3C_2T_x$ MXene, with Cl originating from surface terminations introduced during etching.

Spectral transmittance was measured with a T700S UV-Vis spectrophotometer using a 10 mm quartz cuvette. The transmittance of MXene nanofluids at two different concentrations as a function of wavelength is shown in Figure 3. The average transmittance of the 0.0005 wt% and 0.001 wt% MXene nanofluids was approximately 89.22% and 78.91%, respectively, corresponding to a relative decrease of 11.56%. The higher transmittance of the 0.0005 wt% MXene nanofluid allows a greater portion of incident radiation to reach the underlying PV cell, whereas the stronger optical attenuation of the 0.001 wt% MXene nanofluid increases the interception of incident radiation within the filtering layer.

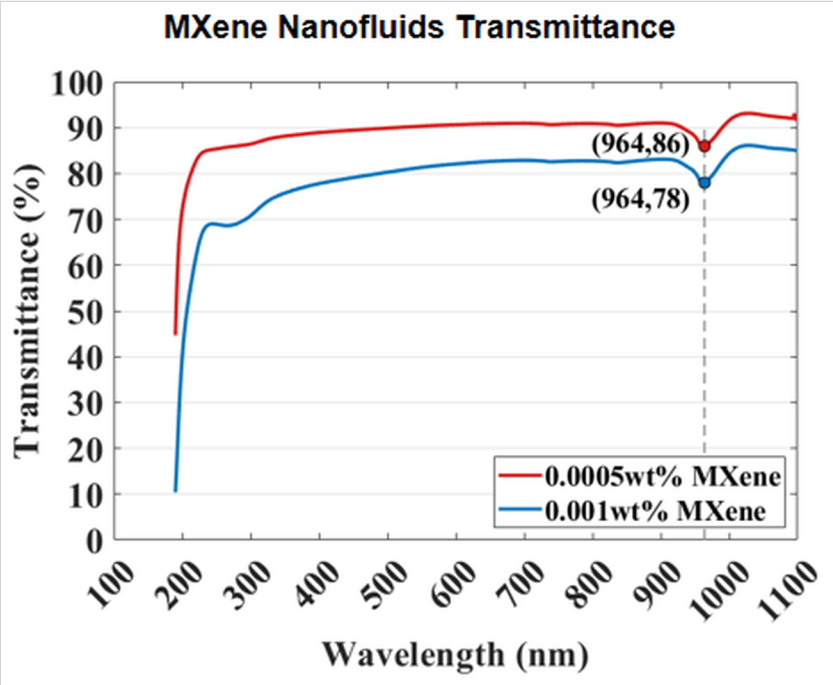

Figure 3. Spectral transmittance of MXene/water nanofluids at concentrations of 0.0005 wt% and 0.001 wt% as a function of wavelength.

Thermal conductivity was measured with a TEMPOS analyser using a KS-3 sensor after glycerin calibration. Each reported value was averaged from three measurements. Specific heat capacity was measured by a DSC 3500 Sirius instrument using the sapphire comparison method, a 10 °C min^{-1} heating rate and a nitrogen flow of 20 mL min^{-1}. The test results are shown in Table 1.

Table 1. Thermal physical properties.

Type	Location	Specific heat capacity (J/kg·K)	Thermal conductivity (W/m·K)
0.0005 wt% MXene	OFL	4179 (25 °C)	0.616
0.001 wt% MXene	OFL	4179 (25 °C)	0.619
0.1 wt% MXene	HTF	4178 (25 °C)	0.630

3. Solar PV/T experimental platform

3.1. Indoor experimental test

The indoor layout is shown in Figure 4 and includes (1) solar simulator, (2) PV/T with OFL module, (3) BD100 unidirectional DC transmitter, (4) data taker, (5) peristaltic pump, (6) constant temperature water tank, (7) heat exchanger, and (8) computer. A solar simulator illuminated the module continuously for 60 min in each test. Electrical signals and inlet, outlet and surface temperatures were acquired to compare the response of each filter medium at each thickness. The pump circulated the rear heat-transfer fluid through the module, heat exchanger and temperature-controlled tank. While keeping the fluid concentration on the dorsal side constant, three types of OFL media were compared, and the optimal configuration for OFL concentration and thickness was determined.

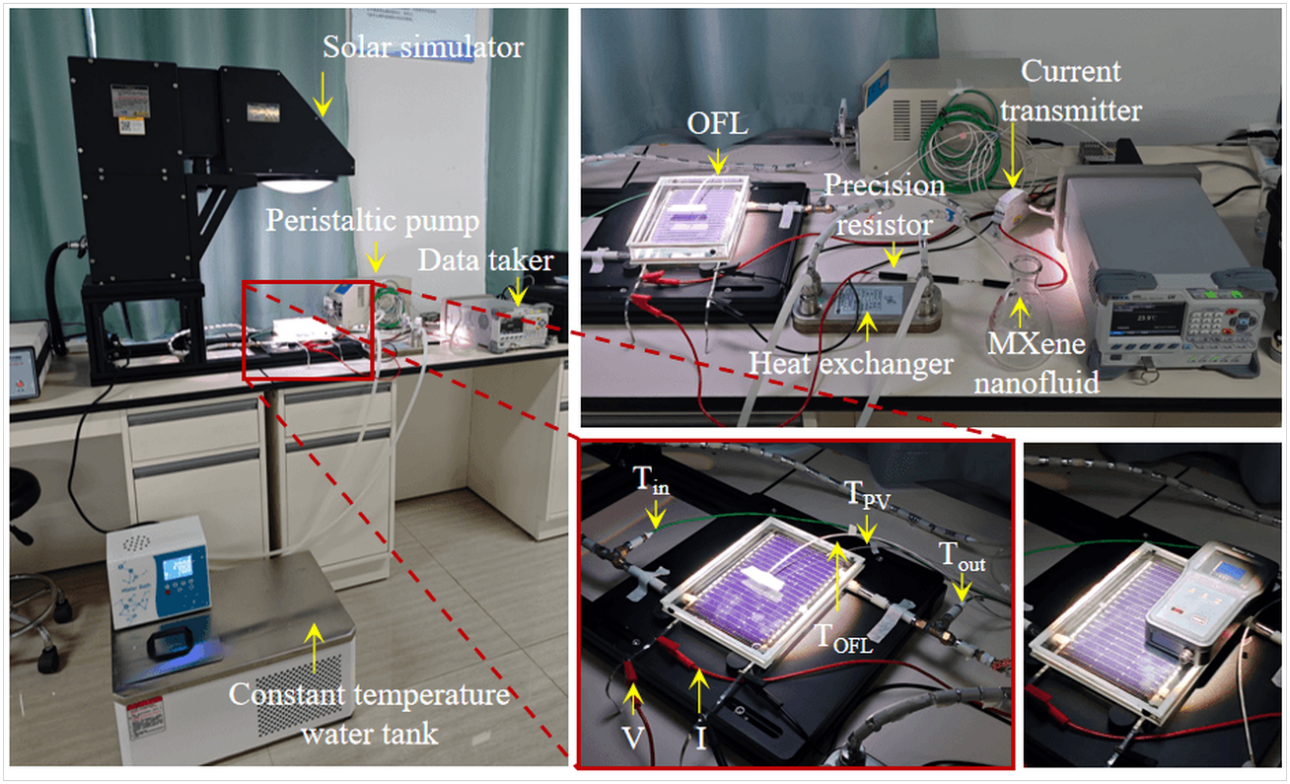

Figure 4. Actual image of indoor experimental test.

In the experiment, the MXene nanofluid serves as heat transfer fluid. The thickness and concentration of OFL are individually varied to test the PV cell temperature and the electro-thermal efficiency of the hybrid PV/T system. The thickness of the OFL above the PV cells is 1, 3, and 5 cm, respectively. The OFL consists of water, 0.0005 wt% MXene, and 0.001 wt% MXene.

4. Power efficiency and uncertainty assessment

To evaluate the impact of the presence of optical filtration layers on the overall PV/T system performance, the measurement data are expressed using two key indicators: electrical efficiency (η_{ele}) and thermal efficiency (η_{th}). Electrical efficiency refers to the efficiency of converting light energy into electrical energy, which is the ratio of output electrical power to input light power (Yadav *et al.* 2024).

$$\eta_{\text{ele}} = \frac{P}{G \cdot A_{\text{pv}}} \times 100\% \tag{1}$$

Where:

- η_{ele} = electrical efficiency (%)
- P = actual output electrical power (W)
- G = solar irradiance (W/m^2)
- A_{PV} = area of the PV cell (m^2)

The thermal energy collected by the PV/T system can be expressed as (Rahmanian and Hamzavi 2020):

$$\eta_{\text{th}} = \frac{c_p \cdot \dot{m} \cdot (T_{\text{out}} - T_{\text{in}})}{G \cdot A_{\text{pv}}} \times 100\% \tag{2}$$

Where:

- η_{th} = thermal efficiency (%)
- c_p = specific heat of fluid (J/kg K)
- $\dot{m}$ = mass flow rate of fluid (kg/s)
- T_{out} = outlet temperature (°C)
- T_{in} = inlet temperature (°C)
- G = solar irradiance (W/m^2)
- A_{PV} = area of the PV cell (m^2)

Therefore, the overall efficiency of the PV/T module is expressed as (Taylor *et al.* 2012):

$$\eta_{\text{overall}} = \eta_{\text{th}} + \eta_{\text{ele}} \tag{3}$$

Where:

- $\eta_{overall}$ = overall efficiency (%)
- η_{th} = thermal efficiency (%)
- η_{ele} = electrical efficiency (%)

Uncertainty analysis of experiments is used to assess the reliability and accuracy of experimental results. For a calculated parameter R = f(x_1, x_2, ..., x_i), the combined uncertainty can be expressed as (Srinivasan and Ponnusamy 2025):

$$U_R = \sqrt{\sum_{i=1}^{n} \left(\frac{\partial R}{\partial x_i} U_{x_i} \right)^2} \tag{4}$$

Where:

- n = total number of input variables
- x_i = the *i*th input variable
- R = calculated quantity
- U_{x_i} = absolute uncertainty of x_i
- U_R = combined uncertainty of R

The calculated uncertainties of the electrical and thermal performance parameters remained within acceptable ranges, indicating that indoor experimental measurements were sufficiently reliable for the subsequent performance comparison and analysis.

5. Indoor results and discussions

5.1. Coupling effects of MXene concentration and OFL thickness on temperature variation

Figure 5(a)(b) shows the average PV and OFL surface temperatures over 60 min. At an OFL thickness of 1 cm, the average PV surface temperatures for water, 0.0005 wt% MXene, and 0.001 wt% MXene were 35.0, 36.5, and 36.4 °C, respectively. Both MXene configurations exhibited higher temperatures than water. At 3 cm, the corresponding temperatures decreased to 32.8, 33.8, and 32.3 °C. The 0.001 wt% MXene configuration was therefore 0.5 and 1.5 °C cooler than water and 0.0005 wt% MXene, respectively. At 5 cm, the temperatures decreased further to 32.0, 31.9, and 30.0 °C, increasing these differences to 2.0 and 1.9 °C. Thus, the PV cooling effect of the higher-concentration MXene nanofluid became more pronounced at greater OFL thicknesses.

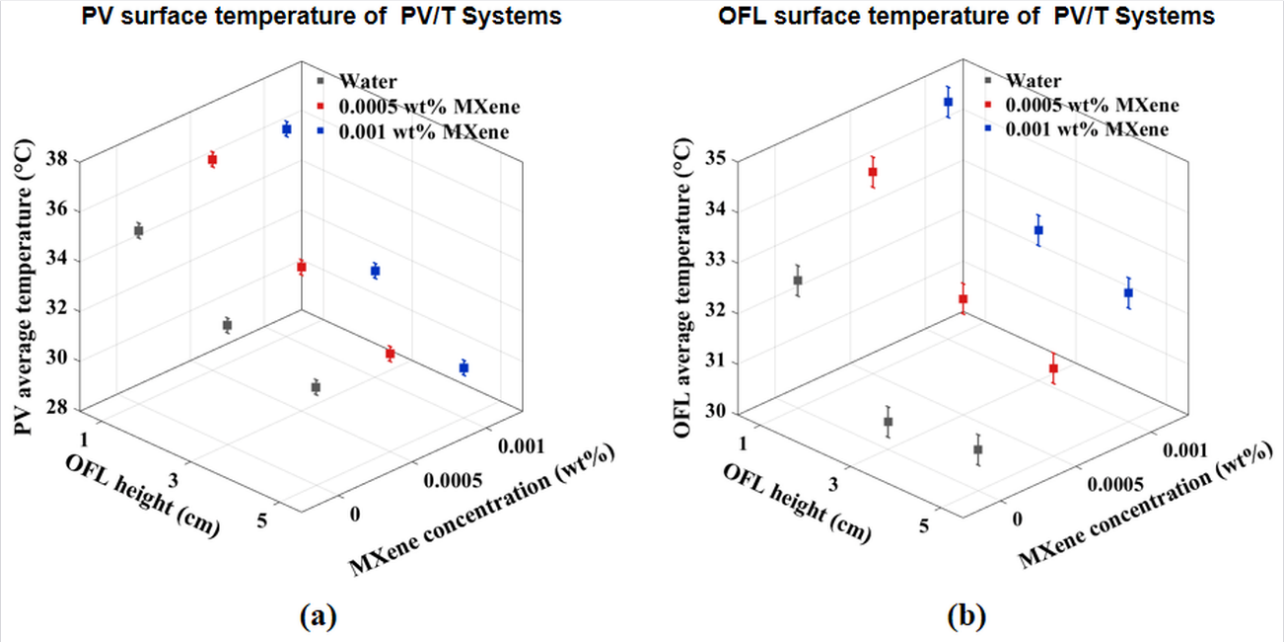

Figure 5. Effect of MXene concentration and optical filter layer thickness on temperature: (a) PV surface average temperature (b) OFL average temperature.

The OFL surface temperature, however, increased with MXene concentration. As shown in Figure 5(b), the average OFL surface temperatures for water and the two MXene concentrations were 32.5, 34.0, and 34.7 °C at 1 cm, respectively. The corresponding values were 30.8, 32.3, and 33.0 °C at 3 cm and 30.5, 31.7, and 32.5 °C at 5 cm. The 0.001 wt% MXene nanofluid consistently exhibited the highest temperature, exceeding water by 2.2, 2.2, and 2.0 °C at the three thicknesses. Increasing OFL thickness from 1 to 5 cm reduced the average OFL temperatures by 2.0, 2.3, and 2.2 °C for water and the two MXene concentrations, respectively.

These trends are consistent with the combined effects of optical attenuation and fluid thermal mass. Increasing MXene concentration enhanced radiation absorption within the filtering medium, raising the OFL temperature. Increasing OFL thickness extended the optical path length and reduced the radiation reaching the PV surface, making PV cooling more pronounced at the higher concentration. Meanwhile, the greater fluid thermal mass of a thicker OFL limited its temperature rise during the experimental period. Consequently, at greater OFL thicknesses, the higher-concentration MXene nanofluid exhibited a warmer filtering layer and a cooler underlying PV surface.

5.2. Effect of MXene concentration and filter thickness on electrical power output and efficiency

As shown in Figure 6, at each fixed OFL thickness, both electrical power and electrical efficiency decreased with increasing MXene concentration. At 1 cm, water, 0.0005 wt% MXene, and 0.001 wt% MXene produced electrical powers of 1.24, 1.14, and 0.72 W, with efficiencies of 9.4468%, 8.6801%, and 5.4820%, respectively. Relative to water, the two MXene configurations reduced electrical power by 8.06% and 41.94% and electrical efficiency by 8.12% and 41.97%. At 3 cm, the corresponding powers were 1.05, 0.81, and 0.19 W, while efficiencies were 7.9978%, 6.1548%, and 1.4834%. The power reductions relative to water increased to 22.86% and 81.90%, accompanied by efficiency reductions of 23.04% and 81.45%. At 5 cm, electrical powers decreased to 0.87, 0.51, and 0.06 W, with efficiencies of 6.6042%, 3.8723%, and 0.4517%. Compared with water, the two MXene configurations reduced power by 41.38% and 93.10% and efficiency by 41.37% and 93.16%. These results indicate that the electrical penalty associated with increasing concentration became more pronounced at greater OFL thicknesses, consistent with stronger attenuation of radiation reaching the PV cells.

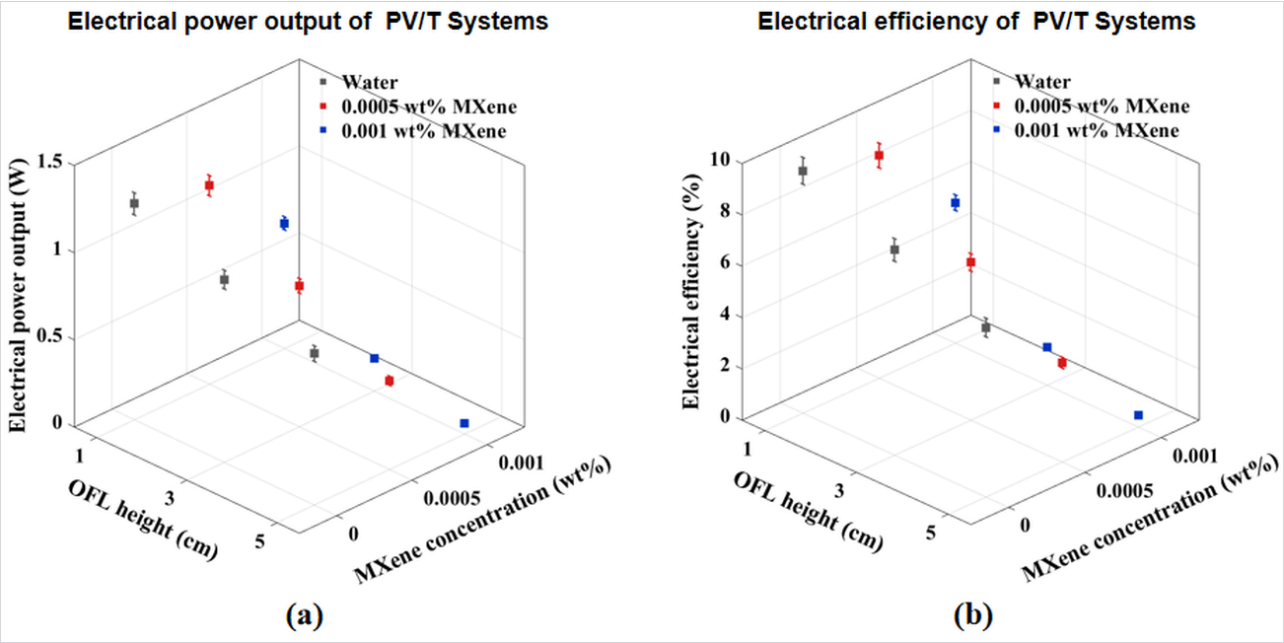

Figure 6. Effect of MXene concentration and optical filter layer thickness on the electrical performance of the PV/T system: (a) electrical power output and (b) electrical efficiency.

Increasing OFL thickness reduced electrical power and efficiency for all three media. When thickness increased from 1 to 3 cm, electrical power decreased by 15.32% for water, 28.95% for 0.0005 wt% MXene, and 73.61% for 0.001 wt% MXene. The corresponding efficiency reductions were 15.34%, 29.09%, and 72.94%. Increasing thickness further to 5 cm resulted in power reductions of 29.84%, 55.26%, and 91.67% relative to the respective 1 cm configurations, while efficiency decreased by 30.09%, 55.39%, and 91.76%. The greater thickness sensitivity at higher MXene concentration is consistent with increased optical attenuation over a longer optical path. Although thicker filters could reduce PV heating, this cooling benefit did not compensate for the loss of transmitted radiation. Within the tested range, a 1 cm OFL therefore provided the highest electrical power and efficiency for each medium.

5.3. Effect of MXene concentration and filter thickness on thermal power output and efficiency

Figure 7 shows that increasing MXene concentration did not consistently improve thermal performance. At an OFL thickness of 1 cm, water, 0.0005 wt% MXene, and 0.001 wt% MXene produced

thermal powers of 3.92, 4.28, and 4.17 W, with thermal efficiencies of 29.902%, 32.694%, and 31.813%, respectively. Relative to water, the two MXene configurations increased thermal power by 9.18% and 6.38% and thermal efficiency by 9.34% and 6.39%. The dilute filter therefore provided the greatest useful heat recovery at this thickness. At 3 cm, the corresponding thermal powers were 3.26, 3.41, and 2.86 W, while efficiencies were 24.886%, 26.027%, and 21.810%. Compared with water, 0.0005 wt% MXene increased thermal power and efficiency by 4.60% and 4.58%, whereas 0.001 wt% MXene reduced them by 12.27% and 12.36%. At 5 cm, thermal powers decreased to 2.96, 2.89, and 2.00 W, with efficiencies of 22.608%, 22.043%, and 15.232%. Both MXene configurations performed below water, with power reductions of 2.36% and 32.43% and efficiency reductions of 2.50% and 32.63%, respectively.

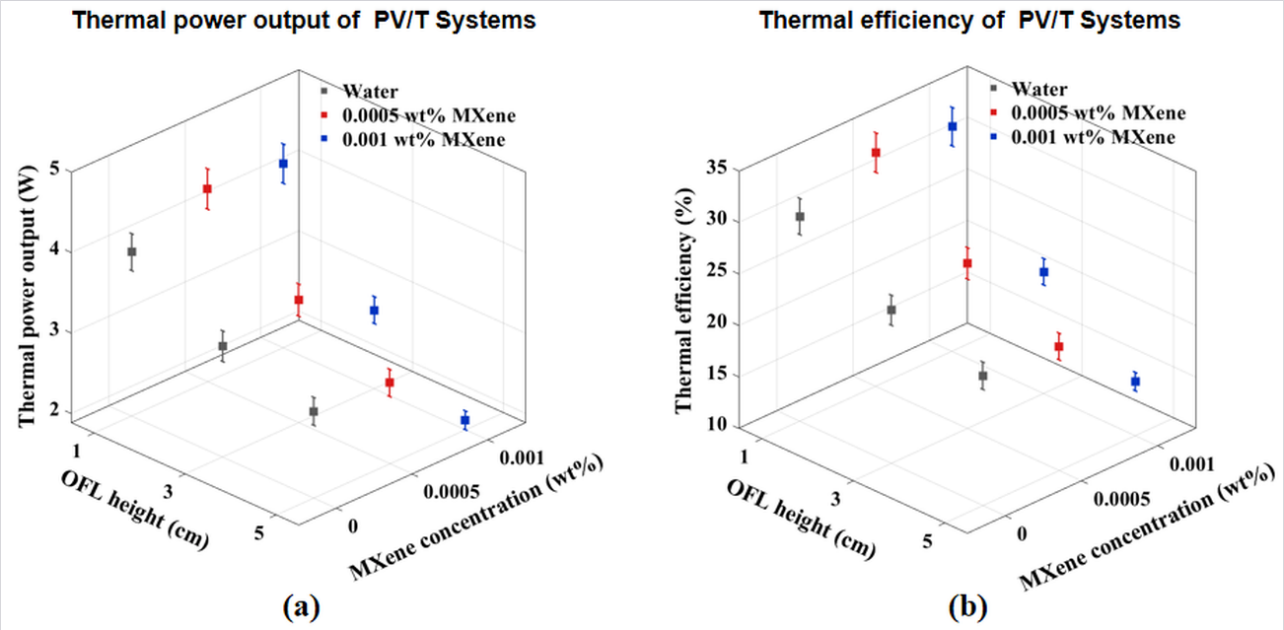

Figure 7. Effect of MXene concentration and optical filter layer thickness on the thermal performance of the PV/T system: (a) thermal power output and (b) thermal efficiency.

Increasing OFL thickness reduced useful thermal power and thermal efficiency for all three media. When thickness increased from 1 to 5 cm, thermal power decreased by 24.49% for water, 32.48% for 0.0005 wt% MXene, and 52.04% for 0.001 wt% MXene. The corresponding thermal-efficiency reductions were 24.39%, 32.58%, and 52.12%. The greater reduction at higher concentration indicates that stronger filtration did not necessarily improve useful heat recovery. A thicker OFL increases both the optical path length and fluid thermal mass, which can change the distribution of absorbed radiation and delay heat transfer during the test. Radiation absorbed within the OFL was therefore not necessarily recovered through the rear cooling circuit. Within the tested range, the 1 cm, 0.0005 wt% MXene configuration provided the highest thermal power and thermal efficiency.

5.4. Effect of MXene concentration and filter thickness on overall power output and efficiency

The overall energy performance was evaluated by combining the electrical and useful thermal outputs. At an OFL thickness of 1 cm, water, 0.0005 wt% MXene, and 0.001 wt% MXene achieved overall powers of 5.16, 5.42, and 4.89 W, with overall efficiencies of 39.35%, 41.37%, and 37.30%, respectively. Compared with water, 0.0005 wt% MXene increased overall power by 5.04% and overall efficiency by 5.15%. Its thermal-power gain of 0.36 W exceeded its electrical-power loss of 0.10 W, resulting in a net improvement of 0.26 W. In contrast, 0.001 wt% MXene reduced overall power and

overall efficiency by 5.23% and 5.22%, respectively, because its thermal improvement was insufficient to compensate for the electrical loss. At 3 cm, the corresponding overall powers were 4.31, 4.22, and 3.05 W, with overall efficiencies of 32.88%, 32.18%, and 23.29%. Relative to water, the two MXene configurations reduced overall power by 2.09% and 29.23% and overall efficiency by 2.13% and 29.16%. At 5 cm, overall powers decreased to 3.83, 3.40, and 2.06 W, while overall efficiencies fell to 29.21%, 25.92%, and 15.68%, respectively. Both MXene configurations performed below water, with overall-power reductions of 11.23% and 46.21% and overall-efficiency reductions of 11.29% and 46.31%.

Increasing OFL thickness reduced overall power and overall efficiency for all three media. When thickness increased from 1 to 5 cm, overall power decreased by 25.78% for water, 37.27% for 0.0005 wt% MXene, and 57.87% for 0.001 wt% MXene. The corresponding overall-efficiency reductions were 25.76%, 37.36%, and 57.95%. These results show that the benefit of MXene addition depended on both concentration and OFL thickness. At 1 cm, the thermal improvement provided by the dilute nanofluid compensated for its relatively small electrical loss. At greater thicknesses, stronger optical attenuation reduced electrical generation, while useful thermal recovery also declined. Therefore, stronger absorption within the OFL did not necessarily improve overall energy performance. Within the tested range, the 1 cm, 0.0005 wt% MXene configuration provided the most favorable electrical–thermal balance, achieving the highest overall power of 5.42 W and overall efficiency of 41.37%.

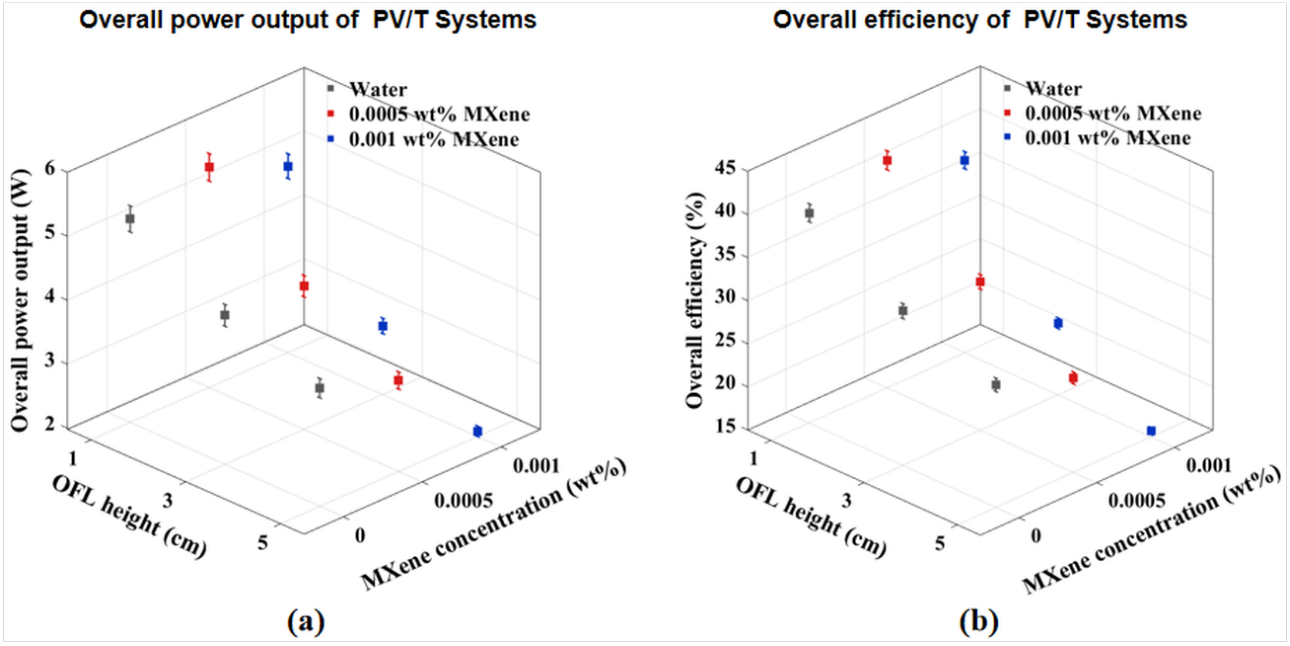

Figure 8. Effect of MXene concentration and optical filter layer thickness on the overall performance of the PV/T system: (a) overall power output and (b) overall efficiency.

6. Conclusion

In this investigation, the authors developed a MXene nanofluid-based spectral filtering PV/T system and experimentally evaluated the effects of MXene concentration (0.0005 wt% and 0.001 wt%) and optical filtering layer thickness (1, 3, and 5 cm) on the photovoltaic performance, thermal energy recovery capability, and overall energy conversion efficiency of the system. By analyzing solar spectrum modulation and heat transfer behavior, the authors uncovered the mechanisms through

which MXene concentration and filtering layer thickness influence the energy conversion performance of the PV/T system. The main conclusions were summarized as follows:

- The MXene concentration and OFL thickness jointly determine the balance between electrical and thermal performance. A lower PV surface temperature resulting from stronger optical attenuation does not necessarily improve electrical efficiency.
- The optical filtering layer thickness significantly influenced the distribution of solar energy between photovoltaic conversion and thermal energy recovery. Increased OFL thickness reduced electrical output and useful thermal recovery under the tested conditions, while generally lowering the average PV surface temperature.
- MXene concentration exhibited a dual influence on the performance of the PV/T system. An appropriate MXene concentration enhanced solar spectral absorption and improved thermal energy utilization, whereas excessive MXene loading caused excessive optical attenuation and reduced the solar radiation available for photovoltaic conversion. At OFL thickness of 1 cm, within the investigated concentration range, the 0.0005 wt% MXene nanofluid achieved a favorable balance between thermal enhancement and electrical output preservation, while the 0.001 wt% MXene nanofluid resulted in a considerable reduction in photovoltaic performance due to excessive optical absorption.
- At OFL thickness of 1 cm, a filtration layer with a concentration of 0.0005 wt% yields an electrical power of 1.14 W and a thermal power of 4.28 W, resulting in a total power of 5.42 W. Compared to pure water, the thermal power increases by approximately 9.2%, which compensates for an 8.1% loss in electrical power, leading to an overall increase in overall power of approximately 5.0%.
- The experimental results primarily reflect system performance under the specified irradiation conditions and during the test period, limiting a comprehensive assessment of the effects of solar irradiance and ambient temperature. Future studies could extend the testing duration and incorporate outdoor experiments under variable natural solar irradiation to further clarify the relationship between optical attenuation and useful thermal recovery.

Declarations

Author contributions. Ziyan Sun: Writing (original draft), Methodology. Xianlong Shi: Data curation. Yuanlong Cui: Methodology, Supervision, Conceptualization.

Funding. This work was financially supported by the Natural Science Foundation Project of Shandong Province (Project Number: ZR2023ME121).

Conflicts of interest. The authors declare no competing interests.

Data availability. The data that support the findings of this study are available from the corresponding author upon reasonable request.

References

Anwer, Shoaib; Alazzam, Anas; Abu-Nada, Eiyad (2025) 'Engineering and Optimization of Stable 2-Dimensional MXene-Based Nanofluid for Direct Absorption Photothermal Energy Conversion', *Energy Material Advances*, 6, pp. 0153. Available at: https://doi.org/10.34133/energymatadv.0153

Cai, Yong; Dai, Yuying; Ma, Yue; Wang, Gang; Xu, Guanghui; Ren, Xingang; Wang, Hui; Zhao, Xiaohu; Wu, Xianliang (2025) 'Optically transparent transmissive orbital angular momentum (OAM) metasurface with high transmittance and broadband characteristics', *Optics Express*, 33(12), pp. 24385. Available at: https://doi.org/10.1364/oe.560640

Cui, Yuanlong; Tian, Shuangqing; Zhu, Jie (2025) 'Experimental study of liquid optical filtration PV/T modules with different working fluids', *Renewable Energy*, 246, pp. 122893. Available at: https://doi.org/10.1016/j.renene.2025.122893

Cui, Yuanlong; Sun, Ziyan; Wang, Xiaohang; Tian, Shuangqing; Zhu, Jie (2026) 'Numerical and experimental studies of a hybrid PV/T module with optical filtration layer for efficient solar energy harvesting', *Energy*, 362, pp. 142199. Available at: https://doi.org/10.1016/j.energy.2026.142199

Dashtbozorg, Amirhosein; Safarianbana, Behnaz; Shanbedi, Mehdi (2025) 'Enhancing PV/T systems performance: A comprehensive study on MXene/methanol nanofluid in two-phase closed thermosyphons', *Solar Energy Materials and Solar Cells*, 279, pp. 113274. Available at: https://doi.org/10.1016/j.solmat.2024.113274

Herrando, María; Wang, Kai; Huang, Gan; Otanicar, Todd; Mousa, Osama Bany; Agathokleous, Rafaela A.; Ding, Yulong; Kalogirou, Soteris; Ekins-Daukes, Ned; Taylor, Robert A.; Markides, Christos N. (2023) 'A review of solar hybrid photovoltaic-thermal (PV-T) collectors and systems', *Progress in Energy and Combustion Science*, 97, pp. 101072. Available at: https://doi.org/10.1016/j.pecs.2023.101072

Jiao, Yue; Xing, Meibo; Estellé, Patrice (2024) 'Efficient utilization of hybrid photovoltaic/thermal solar systems by nanofluid-based spectral beam splitting: A review', *Solar Energy Materials and Solar Cells*, 265, pp. 112648. Available at: https://doi.org/10.1016/j.solmat.2023.112648

Lee, Jae Won; Song, Min Soo; Jung, Han Sol; Kang, Yong Tae (2023) 'Development of solar radiation spectrum-controlled emulsion filter for a photovoltaic-thermal (PVT) system', *Energy Conversion and Management*, 287, pp. 117087. Available at: https://doi.org/10.1016/j.enconman.2023.117087

Rahmanian, S.; Hamzavi, A. (2020) 'Effects of pump power on performance analysis of photovoltaic thermal system using CNT nanofluid', *Solar Energy*, 201, pp. 787-797. Available at: https://doi.org/10.1016/j.solener.2020.03.061

Rubbi, Fazlay; Habib, Khairul; Saidur, R.; Aslfattahi, Navid; Yahya, Syed Mohd; Das, Likhan (2020) 'Performance optimization of a hybrid PV/T solar system using Soybean oil/MXene nanofluids as A new class of heat transfer fluids', *Solar Energy*, 208, pp. 124-138. Available at: https://doi.org/10.1016/j.solener.2020.07.060

Sanjeevi, Baskar; Loganathan, Karikalan (2020) 'Synthesis of multi wall carbon nanotubes nanofluid by using two step method', *Thermal Science*, 24(1 Part B), pp. 519-524. Available at: https://doi.org/10.2298/tsci190414430s

Srinivasan, Nanda kumar; Ponnusamy, Chandrasekaran (2025) 'Impact of surfactant groups on the stability, thermophysical and phase change characteristics of water-based single and hybrid nanofluid PCMs for cool energy storage applications', *Thermal Science and Engineering Progress*, 59, pp. 103298. Available at: https://doi.org/10.1016/j.tsep.2025.103298

Taylor, Robert A; Otanicar, Todd; Rosengarten, Gary (2012) 'Nanofluid-based optical filter optimization for PV/T systems', *Light: Science & Applications*, 1(10), pp. e34-e34. Available at: https://doi.org/10.1038/lsa.2012.34

Wang, Hao; Li, Xiaoke; Luo, Boqiu; Wei, Ke; Zeng, Guangyong (2021) 'The MXene/water nanofluids with high stability and photo-thermal conversion for direct absorption solar collectors: A comparative study', *Energy*, 227, pp. 120483. Available at: https://doi.org/10.1016/j.energy.2021.120483

Wang, Gang; Liu, Jialin; Zou, Tianlin; Han, Wei; Chen, Zeshao (2025) 'Design and performance evaluation of a novel solar concentration PVT system with dual-runner nanofluids optical filtering', *Energy*, 340, pp. 139259. Available at: https://doi.org/10.1016/j.energy.2025.139259

Xia, Xiaokang; Cao, Xuhui; Li, Niansi; Yu, Bendong; Liu, Huifang; Ji, Jie (2023) 'Study on a spectral splitting photovoltaic/thermal system based on CNT/Ag mixed nanofluids', *Energy*, 271, pp. 127093. Available at: https://doi.org/10.1016/j.energy.2023.127093

Xing, Meibo; Jiao, Yue; Chen, Hongbing (2024) 'Tunable electrical/thermal output performance of the PV/T system with magnetic nanofluid based spectral beam filter', *Energy Conversion and Management*, 319, pp. 118951. Available at: https://doi.org/10.1016/j.enconman.2024.118951

Yadav, Satish Kumar; Vishnu Varma, K.S.; Khatoon, Sidra; Chakraborty, Vishwadeep; Singh, Jyotsna; Singh, Rajendra Bahadur; Hasnain, S.M. Mozammil; Zairov, Rustem (2024) 'Ray tracing design-optimization & experimental validation of water based optical filter to reduce solar PV module heating', *Case Studies in Thermal Engineering*, 63, pp. 105271. Available at: https://doi.org/10.1016/j.csite.2024.105271

Zeng, Wengao; Ye, Xiaoyuan; Dong, Yuchen; Zhang, Yuqi; Sun, Chengzhuo; Zhang, Tuo; Guan, Xiangjiu; Guo, Liejin (2024) 'MXene for photocatalysis and photothermal conversion: Synthesis, physicochemical properties, and applications', *Coordination Chemistry Reviews*, 508, pp. 215753. Available at: https://doi.org/10.1016/j.ccr.2024.215753

HOW TO CITE THIS PAPER

Sun, Z., Shi, X. and Cui, Y. (2026). Experimental Investigation of the Effects of MXene Concentration and Optical Filter Layer Thickness on PV/T System Performance. In: *Proceedings of the 22nd International Conference on Sustainable Energy Technologies (SET2026)*, Kuala Lumpur, Malaysia, 13 to 15 August 2026. Caravel Press, pp. 82–94. ISBN 978-1-995850-00-9. ISSN 2978-4387. https://doi.org/10.65582/set.2026.007

COPYRIGHT AND LICENCE

© 2026 The Author(s). This is an open access paper distributed under the terms of the Creative Commons Attribution (CC BY 4.0) licence, which permits unrestricted use, distribution and reproduction in any medium, provided the original work is properly cited.

WSSET World Society of Sustainable Energy Technologies Organised by the World Society of Sustainable Energy Technologies. Published by Caravel Press.